A Study on Factors Affecting Combustion Characteristics of GCSC Injector

동축형 분사기의 연소 특성에 영향을 주는 인자에 관한 연구

저자
(Authors)

Yuangang Wang, Jinwoo Son, Chae Hoon Sohn

출처
(Source)

한국연소학회지 24(1), 2019.3, 32-38(7 pages)

Journal of The Korean Society of Combustion 24(1), 2019.3, 32-38(7 pages)

발행처
(Publisher)

한국연소학회
The Korean Society Of Combustion

URL

http://www.dbpia.co.kr/journal/articleDetail?nodeId=NODE07967345

APA Style

Yuangang Wang, Jinwoo Son, Chae Hoon Sohn (2019). A Study on Factors Affecting Combustion Characteristics of GCSC Injector. 한국연소학회지, 24(1), 32-38

J. Korean Soc. Combust. 24(1) (2019) 32-38

《학술논문》 DOI: http://dx.doi.org/10.15231/jksc.2019.24.1.032 ISSN 1226-0959
eISSN 2466-2089

동축형 분사기의 연소 특성에 영향을 주는 인자에 관한 연구

왕위엔강* · 손진우* · 손채훈*†
*세종대학교 기계공학과

A Study on Factors Affecting Combustion Characteristics of GCSC Injector

Yuangang Wang*, Jinwoo Son* and Chae Hoon Sohn*†
*Department of Mechanical Engineering, Sejong University, Korea

(Received 12 November 2018, Received in revised form 2 January 2019, Accepted 10 January 2019)

ABSTRACT

Factors affecting the combustion characteristics of gas-centered swirl coaxial (GCSC) injectors are investigated numerically and experimentally. The factors are fuel volume flow rate (Q_f), momentum flux ratio (MFR) and oxidizer/fuel (O/F) ratio. Firstly, the flame pattern becomes asymmetric as the fuel volume flow rate increases with a fixed momentum flux ratio. Then, the suitable fuel volume flow rate is selected according to the results. Next, the momentum flux ratio is increased by increasing the oxidizer volume flow rate (Q_o) with a fixed fuel volume flow rate. Results show that the spreading angle decreases as momentum flux ratio increases, which agrees with our previous results. Finally, in order to check effects of oxidizer/fuel ratio, the Q_f, Q_o, and MFR are kept the same but the O_2 mole fraction of oxidizer is changed. From numerical and experimental results, it is found that flame pattern depends on oxidizer/fuel ratio and spreading angle increases as the O_2 mole fraction decreases.

Key Words : GCSC injector, Combustion characteristics, Momentum flux ratio

기 호 설 명

MFR : Momentum flux ratio	R : Specific gas constant
MW : Molecular weight	T : Temperature
U : Axial velocity	α : Spreading angle
Q : Volume flow rate	ρ : Density

1. Introduction

The staged combustion cycle has been widely employed in development of rocket engine because it can reduce system loss, increase efficiency and provide higher performance and more thrust[1]. During its development process, high frequency combustion instability observed for high pressure and temperature condition is always a major issue. It is a phenomenon that pressure oscillations are coupled with heat release, and excessive heat transfer is generated as they oscillate in the chamber[2-5]. Lots of previous studies show that the injector is one of key elements and has great impact on combustion instability [6,7]. And, gas-centered swirl coaxial (GCSC) injector is used typically in a liquid rocket engine adopting staged combustion cycle[8-10].

In our previous work, the GCSC injector with kerosene fuel was studied in various aspects. In order to analyze the combustion instability of the GCSC injector with a

†Corresponding Author, chsohn@sejong.ac.kr

subscale chamber, a scaling method was established by keeping hydrodynamics similarity[11]. Based on this, analysis of fuel-oxidizer mixing and combustion was presented by Kim. et al. with a gas-gas injection in GCSC injector[12]. And, also the spray patterns and injection characteristics were investigated[13]. One of the most significant results in our previous research is that the kerosene model condition was established based on actual rocket engine conditions by simulating gas-liquid injection of GCSC injector with gas-gas injection[11,12].

In the present study, the fuel is replaced by methane because experiments can be carried out relatively easily and detailed chemical mechanism for methane is available for the numerical simulation. And, our goal is still to study stability of injector with a combustor. However, before we analyze combustion instability of GCSC injectors with methane, flow and combustion characteristics should be investigated first. Because if flow or flame is unstable, there is a great possibility that combustion instability will occur.

Three important factors of GCSC injectors are studied numerically and experimentally. They are fuel volume flow rate (Q_f), momentum flux ratio (MFR), and oxidizer/fuel (O/F) ratio. The momentum flux ratio is defined as the ratio of oxidizer momentum flux to fuel momentum flux and it is a key parameter controlling fluid flow induced by the GCSC injector. It is formulated in the following section.

2. Methodology

2.1. Numerical model

The geometry and mesh grids of the model chamber with a single GCSC injector is shown in Fig. 1. The model is the same as that in our previous study[12]. Oxidizer in a gas phase is injected axially through the center, whereas fuel is injected tangentially through 8 holes located on A-A and B-B cross sections of the injector. After injection, fuel and oxidizer will be mixed in the recess part with a length of 8 mm. Injector and combustor lengths are 117.2 mm and 393 mm, respectively. In the present study, hybrid mesh grids are adopted and the grid number is about 530,000.

In this study, oxidizer is a mixture of oxygen and nitrogen and fuel is methane. In the actual rocket engine, oxidizer is oxygen with gas phase and fuel is kerosene with

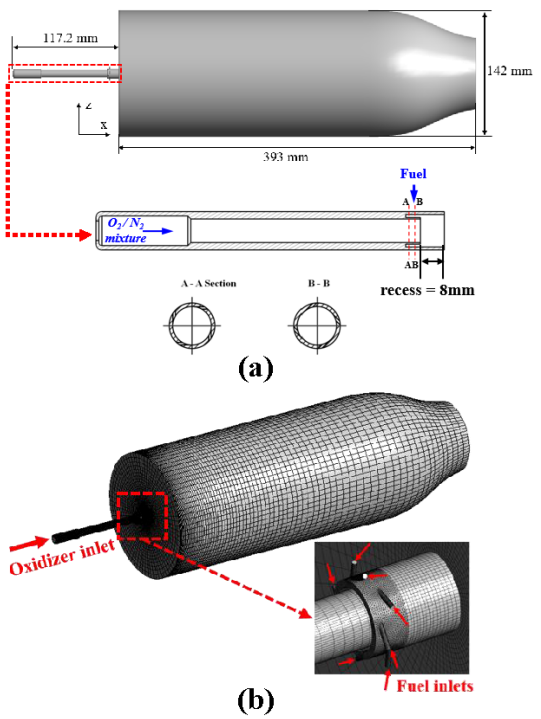

Fig. 1. Geometry and mesh grids of the model chamber with a single GCSC injector.

liquid phase. However, the operating pressure and temperature usually exceed the critical pressure and temperature when fuel and oxidizer are injected into the chamber. That means the process of interaction between fuel and oxidizer inside the injector approaches a gas-gas interacting scheme, not a gas-liquid scheme[12]. When the propellant of rocket engine is gasified, the essential features of gas-liquid flow interaction should be maintained by keeping the hydrodynamic similarity between gas-gas injection and gas-liquid injection. Detail explanation about similarity rules can be found in the literature[13]. In this study, a key parameter controlling fluid flow induced by the GCSC injector is momentum flow ratio (MFR) as describe in Kim et al.'s works[11-13]. The MFR is defined as

$$MFR = \frac{\rho_o U_o^2}{\rho_f U_f^2}, \tag{1}$$

where the subscript, o and f, indicate oxidizer and fuel, respectively. And ρ and U are density and axial velocity.

The method to keep the hydrodynamic similarity and

simulate actual liquid fuel/ gaseous oxidizer with gaseous fuel/ gaseous oxidizer was developed to be a scaling method in our previous study[11,12]. By adopting the scaling method, the gas kerosene/ gas oxygen model condition is calculated. Based on the kerosene model condition, methane model condition is calculated in the present study.

As aforementioned, effects of three factors are studied and flow inlet conditions are summarized in Table 1. The kerosene model condition calculated in our previous study is used for a comparative study with methane fuel[12]. We would like to set the same MFR of kerosene cases as the present methane cases. However there is a problem that fuel and oxidizer volume flow rate are variable with a fixed MFR. First of all, we select the fixed MFR for actual operating condition and change fuel volume flow rate (Q_f) to analyze its effect on GCSC injector with methane fuel. By comparing two results with each other, a suitable Q_f can be determined. Then, studies with various MFR and fixed Q_f are conducted to check MFR effect on flame shape and combustion. Finally, in order to analyze *O/F* ratio effects, conditions with various *O/F* ratio and with MFR, Q_o, and Q_f fixed, are established. A reasonable *O/F* ratio is determined for future numerical simulations and experiments after the analysis of *O/F* ratio effects. Detailed conditions for three factors will be shown in the later section.

The governing equations for the simulation in the present study are as follows:

continuity equation,

$$\frac{\partial \rho}{\partial t} + \nabla \cdot (\rho \vec{v}) = 0, \tag{2}$$

momentum equation,

$$\frac{\partial}{\partial t}(\rho \vec{v}) + \nabla(\rho \vec{v}\vec{v}) = -\nabla p + \nabla \cdot (\bar{\bar{\tau}}) + \rho \vec{g} + \vec{F} \tag{3}$$

energy equation,

$$\frac{\partial}{\partial t}(\rho E) + \nabla \cdot (\vec{v}(\rho E + p)) = \nabla \cdot \left(k_{eff} \nabla T - \Sigma_j h_j \vec{J}_j + (\bar{\bar{\tau}}_{eff} \cdot \vec{v})\right) + S_h \tag{4}$$

species equation,

$$\frac{\partial}{\partial t}(\rho Y_i) + \nabla \cdot (\rho \vec{v} Y_i) = -\nabla \cdot \vec{J}_i + R_i \tag{5}$$

and finally, equation of state,

$$\rho = \frac{p}{(R/MW)T}. \tag{6}$$

In order to simulate the turbulent flow, Reynolds-averaged Navier-Stokes (RANS) equations based on k-ε equations are solved by the commercial CFD solver. Methane GRI 3.0 mechanism is adopted and steady diffusion flamelet model is adopted[14,15].

Table 1. Boundary conditions for three considered factors

	Effect of Q_f	Effect of MFR	Effect of *O/F* ratio
Q_o (LPM)	20.7 ~ 111.8	29.5 ~ 60.3	fixed
Q_f (LPM)	5 ~ 27.05	10	10
Oxygen mole fraction	0.7	0.7	0.3 ~ 1.0
Nitrogen mole fraction	0.3	0.3	0 ~ 0.7
O/F ratio	4.5 ~ 8.1	3.9 ~ 8.1	2.5 ~ 7.9
MFR	fixed	6.5 ~ 27.2	fixed

2.2. Experimental setup

Fig. 2 shows the diagram of the experimental setup. Fuel

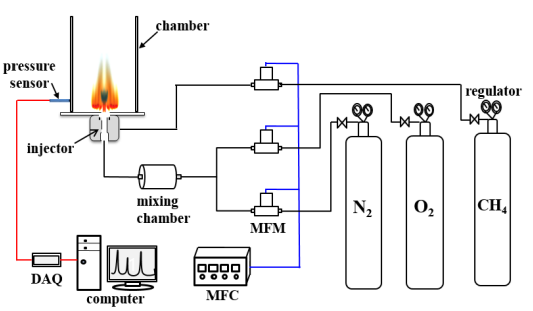

Fig. 2. Schematic diagram of a single GCSC injector experimental setup.

and oxidizer are supplied and controlled by MFC. PCB sensor is installed at the chamber wall to detect pressure fluctuation. In this study, experiments are mainly used to capture flame patterns and to compare flame shape with numerical results.

3. Results and Analysis

3.1. Fuel volume flow rate effect

The methane model condition is calculated based on actual real operating condition by keeping the similar MFR. Since MFR is a ratio between oxidizer and fuel momentum, for a fixed MFR, there will be various combination of fuel and oxidizer volume flow rates. After the fuel is changed to methane, a suitable fuel volume flow rate should be defined. Consequently, the fuel volume flow rate becomes the first factor to be considered. The MFR for the kerosene model condition is set as the baseline value and four different fuel volume flow rates are selected to observe the effect on flow and combustion with the single GCSC injector. The flow conditions are shown in Table 2. The MFR is kept as a similar value to kerosene operating condition. Q_f is increased with the oxidizer flow rate.

Results of numerical simulation with four different Q_f are compared and shown in Fig. 3. When Q_f equals to 27 LPM, which is the same as the Q_f for Kerosene operating condition, the flame shows asymmetric shape as seen in temperature fields. Similarly, with Q_f of 15 LPM, flame is not symmetric. When Q_f is reduced to 10 and 5 LPM, flame becomes symmetric and has stable shape. The fact that flows with larger Q_f show asymmetry can be also found in velocity fields as shown in Fig. 3(b). Next, in Fig. 4, numerical results are compared with experimental results for various Q_f. As in numerical results, larger Q_f also show asymmetry in experimental results. It is because tangential momentum caused by fuel injection larger than axial momentum from oxidizer injection. The large difference between tangential and axial momentum induces the asymmetric flow, resulting in unstable flame. With Q_f of 27 LPM, the axial momentum is too small to form the center flame. Only tangential flame with yellow color can be seen in the figure. When Q_f reduces to 15 LPM, the axial center jet flame can be seen but tangential flame still is asymmetric. In the case of 10 LPM, tangential

Table 2. Flow conditions for numerical study on Q_f effects

	Kerosene	CH_4 (Case1)	CH_4 (Case2)	CH_4 (Case3)	CH_4 (Case4)
Q_o (LPM)	328.7	111.8	62.5	41.1	20.7
Q_f (LPM)	27.0	27.0	15.0	10.0	5.0
MFR	12.2	12.8	12.9	12.6	12.8

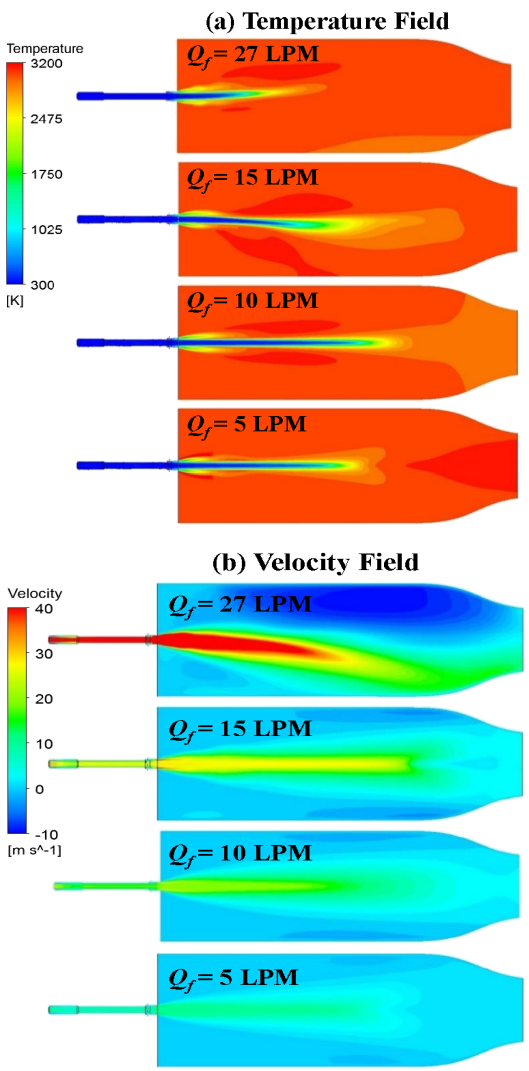

Fig. 3. Temperature and velocity fields calculated with various Q_f.

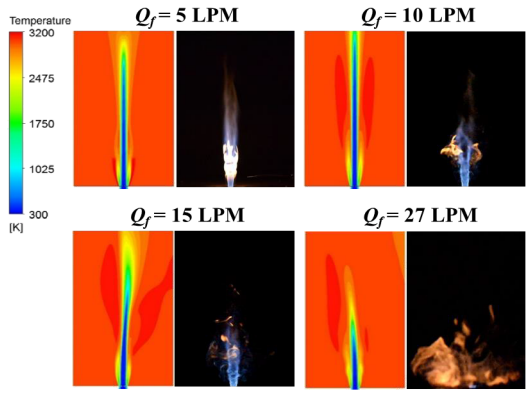

Fig. 4. Comparison of numerical temperature fields with experimental flame shapes for various Q_f.

flame becomes symmetric and stable because tangential momentum decreases. And, the center jet also shows relative stable flow compared with that of larger Q_f. When Q_f decreases further to 5 LPM, central jet flame appears because tangential momentum is too small with little fuel injection. From these flame patterns, 10 LPM is the suitable Q_f and will be adopted in the following simulation and experiments.

3.2. Momentum flux ratio effect

After the fuel volume flow rate Q_f is determined, effect of momentum flux ratio (MFR) is investigated. When the Q_f is fixed at 10 LPM, the MFR can be changed by increasing oxidizer volume flow rate. As shown in Table 3, nine cases with increased MFR are selected and the MFRs for methane are the almost same as those for kerosene in our previous study[12]. The MFR of Test No. 4 is 12.6 which is same as the operating condition in the actual engine. Calculated temperature fields are compared with experimental flame shapes and results in four cases are shown in Fig. 5 with the ascending order of MFR. From the results, we can see that the tangential flame is getting smaller as MFR decreases. In order to quantify this phenomenon, we introduce the parameter of spreading angle characterizing the injection characteristics of GCSC injectors[13]. The spreading angle is calculated by using the Eq. 7,

Table 3. Flow conditions of *MFR* effects

Test No.	1 ~ 9
Q_o (LPM) [for kerosene]	236.1 ~ 482.4 with interval of 30
Q_o (LPM) [for methane]	29.5 ~ 60.3 with interval of 4
Q_f (LPM)	10
MFR [for kerosene]	6.5 ~ 27.2 with interval of 3.2
MFR [for methane]	6.3 ~ 26.3 with interval of 3.2

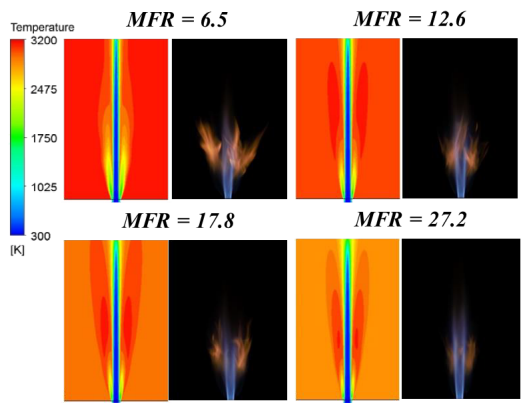

Fig. 5. Comparison of numerical temperature fields with experimental flame shapes for various MFRs.

$$\alpha = \tan^{-1}\left(\frac{Tangential\ Velocity}{Axial\ Velocity}\right). \quad (7)$$

In Fig. 6, the spreading angle of methane fuel is compared with that of kerosene in the previous work. Firstly, the spreading angle of 9 cases decreases as MFR increases. The spreading angle is calculated by numerical results. Although spreading angle cannot be measured with experimental results, the decreasing trend of spreading angle with MFR is confirmed by experimental results as shown in Fig. 5. Spreading angles from both numerical and experimental results show the same qualitative tendancy. Secondly, the error in spreading angle between two fuels is about 17.7%. This is an interesting point to be considered when we determine the flow conditions of GCSC injectors. Because we still need to generate similar flow and combustion pattern to actual condition with any fuels. In

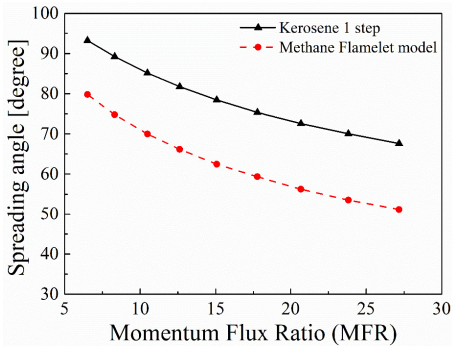

Fig. 6. Spreading angle comparison between kerosene and methane results with various *MFR*.

order to make spreading angles of methane close to that of kerosene we considered the third factor affecting flame shape and flow in next section.

3.3. Oxidizer/Fuel ratio effect

The third parameter is oxidizer/fuel ratio (*O/F* ratio). As aforementioned, the spreading angle between kerosene and methane fuels showed large errors. By comparing the flow condition of kerosene with methane, we found that the *O/F* ratio is different even if we adopt the same MFR. Obviously, MFR is an important factor. But when the oxidizer and fuel volume flow rate is changed to adjust MFR, the *O/F* ratio also should be considered.

The method to change *O/F* ratio is to adjust oxygen and nitrogen mole fraction in oxidizer while the Q_f, Q_o, and MFR are kept constant. Flow conditions are shown in Table 4. Three different *O/F* ratios of 2.5, 5.5 and 7.9 are selected for comparison. The *O/F* ratio 2.5 is similar to that of kerosene. In Fig. 7, flame pattern of kerosene with *O/F* ratio of 2.6 and MFR of 12.2 is shown as a baseline. From the numerical and experimental results, it can be seen that tangential flame appears as *O/F* ratio decreases with MFR fixed in three cases. When the *O/F* ratio of methane has the value 2.5, which is similar to that of kerosene, the spreading angle also becomes similar to each other. As shown In Fig. 8, all of the spreading angle decrease with MFR increases, which agrees with the tendency found in effect of MFR. As *O/F* ratio decreases, the spreading angle of methane increases and is getting close to kerosene. Consequently, the *O/F* ratio with a value of 2.5 will be adopted in our future simulation and experiments.

Table 4. Boundary conditions of *O/F* ratio effects

Test No. 4 (Operating condition)		O_2 mole fraction of Oxidizer (x_{O2})		
		1.00	0.70	0.33
Methane	Q_o (LPM)	41.1	41.1	41.4
	Q_{O2} (LPM)	41.1	28.8	13.7
	Q_{N2} (LPM)	0	12.3	27.7
	Q_f(LPM)	10		
	O/F ratio	7.9	5.5	2.5
	MFR	12.2	12.6	12.2
Kerosene	*O/F* ratio	2.6		
	MFR	12.2		

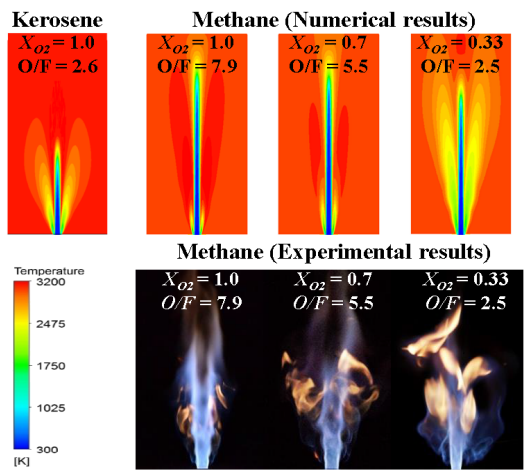

Fig. 7. Numerical and experimental flame patterns for various O/F ratios with MFR fixed.

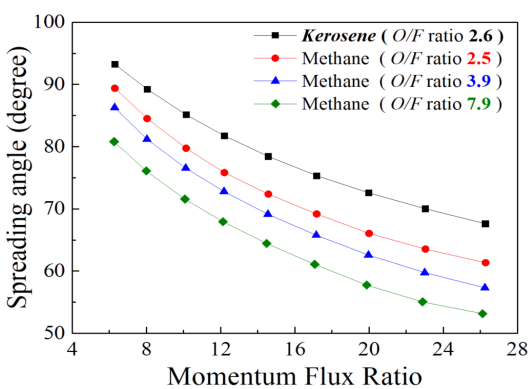

Fig. 8. Spreading angle comparison for each O/F ratio with various *MFR*.

4. Conclusion

Three factors affecting flow and combustion induced by the GCSC injector have been investigated in this study. From the study on Q_f effect, a suitable Q_f was determined for simulation and experiments. And then, the MFR effect have been observed with methane and compared with that of kerosene. The spreading angle decreases with MFR. Finally, in order to get more reasonable flow and combustion fields, the *O/F* ratio effect shoul be considered additionally. A suitable *O/F* ratio was found here and would be applied for our future numerical simulations and experiments with a simulant fuel of methane.

In our future works, the model chamber with single/ multi injectors will be adopted to analyze and predict combustion instability.

Acknowledgement

This work was supported by Advanced Research Center Program (NRF-2013R1A5A1073861) through the National Research Foundation of Korea (NRF) grant funded by the Korea government (MSIP) contracted through Advanced Space Propulsion Research Center at Seoul National University.

References

[1] G.P. Sutton, History of Liquid-Propellant Rocket Engines in Russia, Formerly the Soviet Union, J. Propul. Power, 19 (2003) 1008-1037.

[2] F.E.C. Culick, V. Yang, Overview of Combustion Instabilities in Liquid-Propellant Rocket Engines, Liquid Rocket Engine Combustion Instability, AIAA, Washington, DC, 169 (1995), 3-37.

[3] S. Candel, Combustion Dynamics and Control: Progress and Challenges, Proceedings of the combustion institute, 29, 2002, 1-28.

[4] B.D. Bellows, Y. Neumeier, T. Lieuwen, Forced Response of a Swirling, Premixed Flame to Flow Disturbances, J. Propul. Power, 22 (2006) 1075-1084.

[5] A.P. Dowling, S. Stow, Acoustic Analysis of Gas Turbine Combustors, J. Propul. Power, 19 (2003) 751-764.

[6] K.J. Park, J.Y. Lee, Y.B. Yoon, Study of Gap Thickness in Gas-Centered Swirl Coaxial Injector, KSPE Spring Conference, 2015, 450-453.

[7] J.H. Park, H.J. Kim, An Experimental Assessment of Combustion Stability of Coaxial Swirl Injectors and an Impinging Injector through Simulating Combustion Test, J. Korean Soc. Combust., 22(1) (2017) 46-52.

[8] D.K. Huzel, D.H. Huang, Modern Engineering for Design of Liquid-Propellant Rocket Engines, Prog. Astronaut. Aero., AIAA, Washington, DC, 147 (1992), 35-36.

[9] L. Crocco, Aspects of Combustion Stability in Liquid Propellant Rocket Motors Part I: Fundamentals. Low Frequency Instability With Monopropellants, J. Am. Rocket Soc., 21 (1951) 163-178.

[10] J.W. Son, Y.H. Min, C.H. Sohn, An Experimental Study On Characteristics of Flame and Combustion Stability of Coaxial Jet Injectors, J. Korean Soc. Combust., 21(1) (2016) 15-21.

[11] C.H. Sohn, Y.J. Kim, Y.M. Kim, V.P. Pikalov, A Scaling Method for Combustion Stability Rating of Coaxial Gas-Liquid Injectors in a Subscale Chamber, J. Mech. Sci. Technol., 26 (2012) 3691-3699.

[12] Y.J. Kim, C.H. Sohn, M.G. Hong, S.Y. Lee, An Analysis of Fuel-Oxidizer Mixing and Combustion Induced by Swirl Coaxial Jet Injector with a Model of Gas-Gas Injection, Aerosp. Sci. Technol., 37 (2014) 37-47.

[13] J.W. Son, C.H. Sohn, G.J. Park, Y.B. Yoon, Spray Patterns and Injection Characteristics of Gas-Centered Swirl Coaxial Injectors, J. Aerosp. Eng., 30 (2017) 04017035—1-04017035—8.

[14] ANSYS Fluent Theory Guide, Release 19.1, ANSYS Inc., 2018.

[15] ANSYS Fluent Tutorial Guide, Release 19.1, ANSYS Inc., 2018.